Quantitative Profiling of Ubiquitylated Proteins Reveals Proteasome Substrates and the Substrate Repertoire Influenced by the Rpn10 Receptor Pathway*[S]

Thibault Mayor‡§¶, Johannes Graumann‡, Jennifer Bryan‖, Michael J. MacCoss‡‡§§, and Raymond J. Deshaies‡¶¶¶**

The ubiquitin proteasome system (UPS) comprises hundreds of different conjugation/deconjugation enzymes and multiple receptors that recognize ubiquitylated proteins. A formidable challenge to deciphering the biology of ubiquitin is to map the networks of substrates and ligands for components of the UPS. Several different receptors guide ubiquitylated substrates to the proteasome, and neither the basis for specificity nor the relative contribution of each pathway is known. To address how broad of a role the ubiquitin receptor Rpn10 (S5a) plays in turnover of proteasome substrates, we implemented a method to perform quantitative analysis of ubiquitin conjugates affinity-purified from experimentally perturbed and reference cultures of *Saccharomyces cerevisiae* that were differentially labeled with ^{14}N and ^{15}N isotopes. Shotgun mass spectrometry coupled with relative quantification using metabolic labeling and statistical analysis based on *q* values revealed ubiquitylated proteins that increased or decreased in level in response to a particular treatment. We first identified over 225 candidate UPS substrates that accumulated as ubiquitin conjugates upon proteasome inhibition. To determine which of these proteins were influenced by Rpn10, we evaluated the ubiquitin conjugate proteomes in cells lacking either the entire Rpn10 (*rpn10*Δ) (or only its UIM (ubiquitin-interacting motif) polyubiquitin-binding domain (*uim*Δ)). Twenty-seven percent of the UPS substrates accumulated as ubiquitylated species in *rpn10*Δ cells, whereas only one-fifth as many accumulated in *uim*Δ cells. These findings underscore a broad role for Rpn10 in turnover of ubiquitylated substrates but a relatively modest role for its ubiquitin-binding UIM domain. This approach illustrates the feasibility of systems-level quantitative analysis to map enzyme-substrate networks in the UPS. *Molecular & Cellular Proteomics 6:1885–1895, 2007.*

From the ‡Howard Hughes Medical Institute, Division of Biology, California Institute of Technology, Pasadena, California 91125, §Department of Biochemistry and Molecular Biology, UBC Centre for Proteomics and ‖Department of Statistics, Michael Smith Laboratories, University of British Columbia, Vancouver, British Columbia V6T 1Z4, Canada, and ‡‡Department of Genome Sciences, Health Sciences Center, University of Washington, Seattle, Washington 98195

Received, June 5, 2007

Published, MCP Papers in Press, July 20, 2007, DOI 10.1074/mcp.M700264-MCP200

The classical function of ubiquitylation is to direct substrates for proteolysis via the ubiquitin proteasome system (UPS).[1] Recognition of proteasome substrates is specifically mediated by several receptor proteins (1). In yeast, there are at least five potential receptors (Ddi1, Dsk2, Rad23, Rpn10, and Rpt5) plus a set of Cdc48-based complexes, including the Cdc48-Npl4-Ufd1 heterotrimer, that may possess receptor function (2–7). This diversity of postubiquitylation targeting pathways is mystifying. Currently it is not known which subset of proteasome substrates is targeted by a given receptor or what features govern the allocation of substrates to a particular receptor pathway.

The yeast Rpn10 protein is a stoichiometric component of the 26 S proteasome and was the first protein found to bind polyubiquitin chains (8). Its amino-terminal domain consists of a conserved von Willebrand A (VWA) motif that docks Rpn10 to the proteasome. Recruitment of ubiquitin chains to Rpn10 is mediated by the 20-amino acid ubiquitin-interacting motif (UIM) domain located near its carboxyl terminus (9). S5a protein, the human Rpn10 ortholog, contains a second UIM domain that is thought to mediate the recruitment of other receptor proteins (10). The general impact of Rpn10 on the turnover of proteasome substrates is not known. Given that budding yeast *rpn10*Δ mutants are viable (11, 12), Rpn10 may be required for the turnover of only a small subset of ubiquitylated proteins, or Rpn10 may target a large number of substrates that, in its absence, are targeted by other proteasomal receptors (*e.g.* Rad23 or Dsk2). Even less well understood is the contribution of the two domains of Rpn10 to substrate turnover. Complete deletion of *RPN10* (*i.e. rpn10*Δ) stabilizes the cell cycle regulator Sic1 and the transcription factor Gcn4. Paradoxically removal of the UIM domain by itself (*i.e. uim*Δ) has no discernable effect on either of these substrates (5)[2] suggesting that Rpn10 function may rely solely

[1] The abbreviations used are: UPS, ubiquitin proteasome system; VWA, von Willebrand A; UIM, ubiquitin-interacting motif; FDR, false discovery rate; TAP, tandem affinity purification; MudPIT, multidimensional protein identification technology; WT, wild-type; DUB, deubiquitylating.

[2] J. R. Lipford, personal communication.

on an uncharacterized biochemical activity associated with its VWA domain.

To understand fully the biological roles of protein ubiquitylation and the functions of individual components of the UPS such as Rpn10, it will be necessary to identify UPS substrates on a proteome-wide scale. Several studies have started to address this challenge using mass spectrometry to analyze the ubiquitin proteome (13–18). Although these seminal studies illustrate that shotgun mass spectrometry is a powerful tool that can provide a systems-level view of the ubiquitin proteome, it is clear that application of this technology to the ubiquitin system remains in an embryonic state. For example, no proteomics study has yet succeeded in identifying even one of the 11 yeast G_1 and mitotic cyclins that are well known substrates of the UPS. Indeed many ubiquitin conjugates identified in proteomics experiments might be stably accumulating species that are not substrates of the UPS. To obtain more focused information from shotgun mass spectrometry experiments, we and others have previously applied subtractive approaches to identify conjugates that accumulate in *rpn10*Δ (15) and in *npl4ts* but not *ubc7*Δ mutants (18). Although this strategy allowed the identification of several ubiquitylated proteins, by its nature the subtractive approach excludes substrates whose accumulation is only partially dependent upon a given factor. This is a major concern given the redundancy of many UPS pathways (5, 19). No fewer than six ubiquitin ligases (Mdm2, Pirh2, p300, PARC, Cul7, and Cop1) have been implicated in p53 regulation (20–22), and at least three different ubiquitin chain receptors contribute to turnover of ubiquitylated Sic1 (5). Clearly a method that allows for more subtle quantitative comparisons is needed.

In this study, we adapted stable isotope labeling techniques that have been used previously to address a variety of biological problems to perform relative quantitative analysis of polyubiquitylated proteins in two distinct cell cultures. By applying a statistical approach based on *p* and *q* values, we were able to identify ubiquitylated proteins whose levels are altered in response to a specific perturbation (chemical or genetic). After validating the approach, we used this method to identify putative substrates of the proteasome and to determine the contribution of the Rpn10 proteasome receptor pathway in the targeting of UPS substrates. We further dissected the function of Rpn10 by assessing the role of its UIM domain.

MATERIALS AND METHODS

Strains—All *Saccharomyces cerevisiae* strains used in this study are listed in Supplemental Table 1. RJD2997, which constitutively expresses His_6-ubiquitin, was described previously (23). *PDR5* was deleted to increase sensitivity to the proteasome inhibitor MG132 (24). To obtain a prototrophic strain for labeling with heavy nitrogen, we reverted auxotrophic markers by homologous recombination. The following genes were PCR-amplified using the indicated pair of primers: *ADE2* (5′-TATTAGTGAGAAGCCGAGA, 5′-GATCTTATGTATGAAATTCTT), *LEU2* (5′-TGGTTGTTTGGCCGAGCGG, 5′-TCGACTACGTCGTTAAGGCC), and *URA3* (5′-TCTTAACCCAACTGCACAG, 5′-GTGAGTTTAGTATACATGC). The PCR-amplified fragments were purified and transformed into W303 cells, and revertants were identified by applying the corresponding selection. RJD3313 and -3314 were obtained by successive crosses until all the markers were reverted. Both *rpn10*Δ and *uim*Δ (5) were crossed with RJD3314 to obtain RJD3315 and RJD3318, respectively.

Isotopic Labeling and Two-step Purification—Cells were grown in YNB-D (0.17% yeast nitrogen base without amino acids and ammonium sulfate, 5% dextrose, 20 μg/ml ampicillin) supplemented with 0.5% ammonium sulfate (^{14}N) at 25 °C to an A_{600} between 0.5 and 1, washed three times with YNB-D only, and then diluted to an A_{600} of 0.008 in 2 liters of YNB-D with 0.5% ^{14}N- or ^{15}N-labeled (>98%, Cambridge Isotope Laboratories) ammonium sulfate. The two different isotopically labeled cell cultures were grown in parallel at 25 °C to an A_{600} of 1 (seven generations), and a drug treatment was applied for 30 min where indicated. Each isotopically labeled culture was then harvested by centrifugation and resuspended in 400 ml of ice-cold TBS. The A_{600} was carefully measured, and equal amounts of cells for each isotope variant were mixed together, centrifuged, resuspended in 200 ml of ice-cold TBS with 1 mM 1,10-phenanthroline and 10 mM iodoacetamide, recentrifuged, and snap frozen in liquid nitrogen. The two-step purification and tryptic digestion of ubiquitin conjugates was carried out as described previously (23) with the following minor changes: cells were broken in 40 ml of lysis buffer after which 1.8 mg each of recombinant GST-Rad23 and GST-Dsk2 coupled to Sepharose were used for the first step and 100 μl of nickel magnetic bead slurry (Promega) were used for the second. Typically only one-half of the sample was analyzed in a single LCQ analysis (corresponding to 1 liter of each labeled cell sample), whereas with the LTQ, material corresponding to 500 ml of each labeled culture was analyzed. An aliquot (10 μl) of cleared total cell extract was collected after the first centrifugation, precipitated (25), and resuspended in UB buffer (8 M urea, 100 mM NaH_2PO_4, 10 mM Tris-HCl, pH 8.0). 5 μg of protein were subjected to tryptic digest, mass spectrometry, and quantitative analysis to calculate the average ratio of isotopically labeled proteins in the total cell extract (median of $^{14}N/^{15}N$ ratio values).

Mass Spectrometry Analysis, Computation, and Statistical Analysis—The proteolytically digested proteins analyzed in Fig. 1 were evaluated by multidimensional chromatography coupled in line to ESI-MS using an LCQ-Deca mass spectrometer (ThermoFisher) as described previously (15, 26). Samples in Figs. 3–5 were analyzed with an LTQ ion trap (ThermoFisher) using a modified protocol (supplemental information). Sequest and DTASelect (27, 28) were used to analyze the mass spectrometry profiles using two sets of parameters for ^{14}N and ^{15}N searches (supplemental information). Proteins identified by at least two peptides (Supplemental Table 2) were retained for the quantitative analysis, and peptides (^{14}N and ^{15}N) were separately analyzed with RelEx (versions 0.91 and 0.92 (29)) using the following parameters: (i) width option was ±75 scans with LCQ and ±25 scans with LTQ data; (ii) for purified material, ratio correction was applied using the (median ratio)$^{-1}$ value derived from total cell extract; (iii) regression filter was applied (minimum correlation, 0.7 at 1 and 0.4 at 10); and (iv) signal to noise filter was applied (minimum of 3 for LCQ and 5 for LTQ data). The files from the two separate analyses (^{14}N and ^{15}N) were merged and sorted using RelEx (Supplemental Table 3).

For the purposes of statistical analysis, the $^{14}N/^{15}N$ ratios were analyzed on a base 2 logarithmic scale. Due to a lack of biological interpretability, the following ORFs were removed prior to statistical analysis: YIL148W, YLR167W, YLL039C, and YKR094C (ubiquitin genes); YMR276W and YEL037C (Dsk2 and Rad23, respectively, contaminants from the purification); YML042W, YBR195C, and YGL178W. The background variability (σ^2) of log ratios was estimated from the data observed in the reference experiment (supplemental

information), which specified a null distribution for log ratios, *i.e.* a normal distribution with mean 0 and variance σ^2/n where n is the peptide number. For each ORF quantified in RelEx, the observed log ratio and peptide number were compared with this null distribution to obtain a two-sided p value.

$$p \text{ value (log ratio)} = p(|Z| > \sqrt{n} \times \log(\text{ratio})/\sigma_{\text{ref}}) \text{ where } Z \text{ is } N(0,1) \quad \text{(Eq. 1)}$$

To permit the control of the false discovery rate (FDR) (30) in subsequent lists of putative proteasome substrates, we computed adjusted p values, also known as "q values" (31),

$$q \text{ value } (p_{(i)}) = p_{(i)} \times \pi_0 \times m/i \quad \text{(Eq. 2)}$$

where $p_{(i)}$ is the ith order statistic of the observed p values, π_0 is the (estimated) proportion of unresponsive proteins, and m is the number of proteins quantified. To calculate the recovery rate associated with a q value cutoff equal to $q_{(i)}$, note that, on average, $i \times q_{(i)}$ of the i"discoveries" are false and conversely that $i \times (1 - q_{(i)})$ of the i discoveries are true. Overall $m \times (1 - \pi_0)$ ORFs are thought to be truly responsive; therefore we can estimate the fraction of these that have been recovered in any given list of putative proteasome substrates.

$$\text{Recovery rate } (q_{(i)}) = i \times (1 - q_{(i)})/(m \times (1 - \pi_0)) \quad \text{(Eq. 3)}$$

All statistical analysis was performed using the software environment R (The R Project for Statistical Computing) and the q value package.[3] Analysis scripts are provided in the supplemental information. Frequency distribution, Deming regression, and Fisher's test analyses were performed with Prism 4.0 (GraphPad), and list analysis was performed with Excel (Microsoft) using filter functions.

One-step Purification/Immunoblot Analysis of Ubiquitin Conjugates—For IMAC purification of His_8-ubiquitin, cells transformed with RDB1851 (15), a *URA3*-based plasmid constitutively expressing His_8-ubiquitin, were grown in 100 ml of SD-URA medium (0.67% yeast nitrogen base, 5% dextrose) at 30 °C to an A_{600} of 1 and then treated for 30 min with MG132 (20 μM) or DMSO only (160 μl). Samples were prepared as described previously (15) with the following modifications: trichloroacetic acid was added to a 10% final concentration to the cell cultures, and 50 μl of nickel magnetic bead slurry (Promega) were used. TAP tagged proteins were detected using the anti-calmodulin-binding peptide antibody (Upstate; Fig. 2) or the anti-TAP polyclonal antibody (Open Biosystems; Fig. 4), and Cdc28 was detected for loading control in total cell extract using the PSTAIRE antibody (Santa Cruz Biotechnology).

RESULTS

Quantitative Analysis of Ubiquitin Proteome—The first question we sought to address was to determine which proteins in the ubiquitin proteome are likely to be true UPS substrates as opposed to proteins regulated by ubiquitylation in a non-proteolytic manner or contaminants. Identification of true substrates of the UPS is an important issue because among all the ubiquitylated proteins identified in prior proteomics studies only a handful (*e.g.* Sic1 and Gcn4) correspond to known UPS substrates, and many of the reported proteins are relatively stable. To address this question, we sought a method that would enable us to perform relative quantification against an internal standard of the hundreds of ubiquitylated proteins that are obtained upon affinity purification of ubiquitin conjugates. The general idea was to identify those ubiquitylated proteins that showed elevated accumulation, relative to an internal standard, when the proteolytic activity of the proteasome was chemically inhibited. Multiple methods have been developed to enable quantification (*e.g.* ICAT, SILAC (stable isotope labeling by amino acids in cell culture), iTRAQ (isobaric tags for relative and absolute quantitation), ^{15}N and ^{18}O isotopic labeling, and label-free peak comparison (32)). To exclude variations introduced during the preparation of the samples to be compared (our approach involved a two-step biochemical purification), we opted for biosynthetic labeling with ^{15}N. Yeast cells expressing His_6-tagged ubiquitin and grown in medium provided with normal (^{14}N) nitrogen were incubated with the proteasome inhibitor MG132, whereas the same cells grown in medium formulated with "heavy" (^{15}N) nitrogen were mock-treated (DMSO). The two cultures were then mixed together and lysed, and extracts were subjected to sequential affinity purifications on Rad23-Dsk2 resin and Ni^{2+} magnetic beads as described previously (23). The resulting pool of ubiquitylated proteins was digested with trypsin and subjected to shotgun mass spectrometry (MudPIT) (33) followed by quantitative analysis using RelEx (29). We reasoned that ubiquitylated proteins normally targeted for proteolysis would accumulate in the cells treated with MG132 because they could no longer be degraded. Hence the relative amount of any given ^{14}N-labeled peptide derived from one of these proteins compared with its ^{15}N-labeled isotopomer (*i.e.* the $^{14}N/^{15}N$ ratio) should be greater than 1 (Fig. 1*A*). In contrast, proteins that are not targeted for proteasomal degradation, including proteins conjugated to Lys-63 polyubiquitin chains or contaminating (*i.e.* non-ubiquitylated) material from the purification, should generate ratio values close to 1 (Fig. 1*A*).

To identify proteasome substrates, we had to articulate exactly what constituted compelling evidence that a protein is truly enriched or depleted in the MG132-treated cells. An absolute threshold, such as requiring an observed 2-fold increase or decrease, suffers from two disadvantages. 1) It does not normalize the observed ratio by comparison with the background variability arising purely from biological and experimental noise, and 2) it does not acknowledge the increased confidence that arises when a protein is represented by, for example, 10 distinct peptides as opposed to just three. To avoid these pitfalls, we opted for a statistical approach. The quantitative data taken for each protein is the average log ratio of all sequenced peptides derived from it using a base 2 logarithm. We obtained a "null distribution" of log ratios defined as the distribution of log ratios observed in a reference experiment in which both the ^{14}N- and ^{15}N-labeled cells received the same mock treatment (Fig. 1*B*, *top panel*). Data were obtained for peptides representing 159 different proteins (all quantitative data are provided in Supplemental Table 3). Based on the assumption that log ratios in a null distribution

[3] A. Dabney and J. D. Story, personal communication.

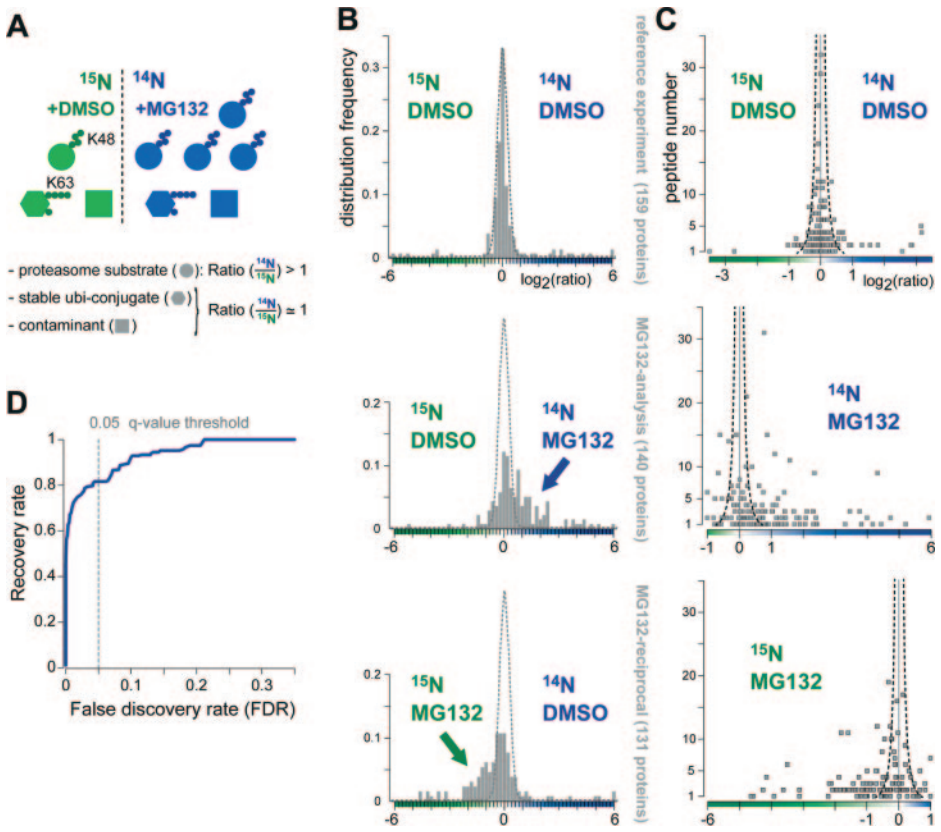

FIG. 1. **Quantitative analysis of the ubiquitin proteome and proteasome substrates.** *A*, schematic representation of the isotopic labeling approach. Two cell populations were separately grown in medium containing ^{14}N (*blue*) or the stable isotope ^{15}N (*green*) for several generations until all proteins were uniformly labeled. The proteasome inhibitor MG132 was applied to cells grown in ^{14}N, whereas ^{15}N-labeled cells were treated with DMSO, the solvent used to dissolve MG132. After ratiometric quantitative mass spectrometry analysis, each identified protein was assessed for its relative enrichment. *B*, frequency distributions of log ratios in the quantitative analyses of the ubiquitin proteome. The *top panel* represents the reference experiment performed using DMSO in both ^{14}N and ^{15}N cells. The *middle panel* corresponds to MG132 analysis in which ^{14}N cells were treated with MG132, and the *lower panel* displays the MG132 reciprocal experiment in which ^{15}N cells were treated. The bell-shaped distribution obtained in the reference experiment is depicted as a *dotted line* in the three panels. *C*, scatter plots of the log ratios and the associated peptide numbers. The analyses are ordered as in *B*. *Points* that lie outside the *dotted lines* deviate from the normal distribution with a *p* value of 0.1 or less. A small number of extreme log ratios are beyond the scale of the horizontal axis and are therefore not depicted here. Note that several proteins were quantified using only one peptide, whereas protein identifications strictly required at least two peptides. *D*, recovery rate (proportion of truly responsive ORFs that are identified) as a function of FDR. The selected *q* value cutoff is depicted in *gray*. Very similar results were obtained in the reciprocal analysis (data not shown).

will be centered at 0, it follows that the null distribution for a protein represented by averaging log ratios from *n* peptides will also be centered at 0 with variance σ^2/n. Our distributional assumptions (normal distribution, centered at 0) and the implied relationship between variance and peptide number (σ^2/n) are consistent with the data observed in the reference experiment (Fig. 1, *B* and *C*, *top panels*). Using an averaging approach that accounted for differences in peptide number (supplemental information), we estimated the variance (σ^2) of the null distribution to be 0.24.

To assess the impact of proteasome inhibition on the composition of the ubiquitin proteome, we treated cells labeled with ^{14}N with the proteasome inhibitor MG132 for 30 min, whereas DMSO was added to ^{15}N control cells. Log ratios were obtained for 140 proteins, and as expected, the observed distribution was shifted toward positive values and was generally more spread out, suggesting that the treatment induced meaningful differences in protein abundance with evidence for a higher prevalence of enrichment (ratios >1 or positive log ratios) than depletion (Fig. 1*B*, *middle panel*; examples of ratio calculation for two ^{14}N-enriched peptides are shown in Supplemental Fig. 1). To evaluate the reproducibility of the ratio measurements and ensure that the enrichment of proteins in the ^{14}N sample was due to the proteasome inhibitor, we performed a "reciprocal" experiment in which MG132 was added to the ^{15}N-labeled cells and DMSO was added to ^{14}N cells. The observed data distribution was as expected with a general shift to negative log ratio values and a much greater range of values relative to the reference experiment (Fig. 1*B*, *bottom panel*). Further evidence of reproducibility is found in the high correlation between the peptide numbers of proteins appearing in both the original MG132

analysis and the reciprocal experiment (Supplemental Fig. 2A). Moreover a Deming regression analysis of the log ratios exhibited by the proteins identified in the two experiments yielded a fit that is compatible with the ideal $x = y$ relationship predicted by theory (Supplemental Fig. 2B). Taken together, this evidence confirms that the MG132 treatment similarly affected ubiquitylation levels of proteins analyzed in both experiments.

For each protein, we obtained a two-sided *p* value by using the null distribution to compute the probability that its log ratio in the MG132 experiment could arise by stochastic fluctuation (Supplemental Table 4). With this approach, one expects that ubiquitylated proteins that are insensitive to MG132 treatment will exhibit *p* values close to 1, whereas ubiquitylated proteins that exhibit robust accumulation upon MG132 treatment will exhibit *p* values close to 0 (in Fig. 1*C* the *dotted lines* indicate log ratios that have an associated *p* value of 0.1). Because we computed and interpreted *p* values for hundreds of proteins simultaneously, it was desirable to adjust them such that by thresholding the adjusted *p* values at some fixed level we could specify an appropriate error rate for the entire collection of *p* values. We used a method of *p* value adjustment that provides control of the FDR (30) defined as the expected proportion of discoveries (*i.e.* proteins claimed to be enriched or depleted due to treatment) that are actually false discoveries (*i.e.* proteins unaffected by treatment). These adjusted *p* values are often called *q* values (31), and a useful and interpretable by-product of the *q* value computation is an estimate of the proportion of studied proteins that are truly unresponsive to the experimental perturbation, often denoted π_0. Further computation also allowed us to estimate the "recovery rate" associated with each potential *q* value cutoff defined as the proportion of proteins that respond to the perturbation that would be discovered. Supplemental Table 4 contains *p* and *q* values, π_0, and recovery rates for all experiments, and Fig. 1*D* represents the results for the MG132-analysis. We chose to set the FDR at the level of 5%, which produces a high quality list of candidates (on average, only 5% will be false "hits") while also promising a very high recovery rate (estimated to be ~80% in both MG132 analysis and reciprocal experiments). To identify those proteins that are the best candidates for proteasome substrates, we then narrowed our focus to proteins enriched in cells treated with MG132 (Supplemental Table 5).

Validation of UPS Substrates—To evaluate the legitimacy of our approach, we sought to validate candidate proteasome substrates using a completely orthogonal method. Yeast cells expressing His_8-ubiquitin and carrying a TAP tagged allele at the endogenous locus of each tested candidate gene were treated with or without MG132, lysed, and subjected to IMAC followed by immunoblotting for the TAP tag (Fig. 2*A*). Control experiments were done in parallel with an untagged strain and in the absence of His_8-ubiquitin expression to evaluate specificity. Upon addition of MG132, increased ubiquitylation was

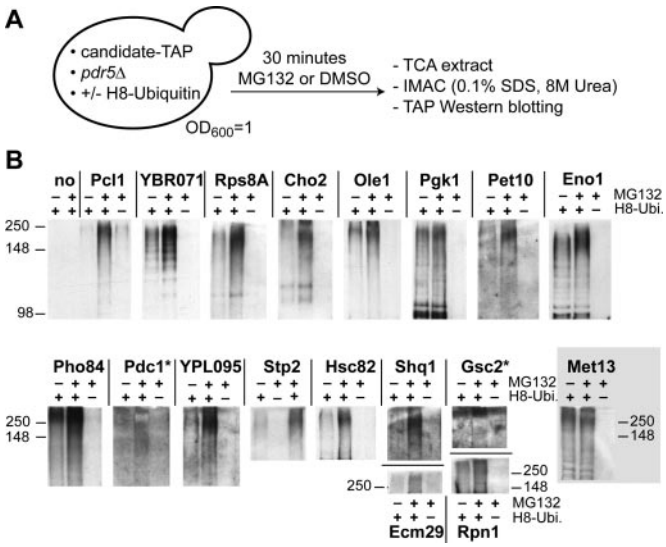

FIG. 2. **Analysis of candidate substrates of the proteasome.** *A*, schematic representation of the validation strategy. *B*, purification of proteins conjugated to His_8-ubiquitin. Strains with the indicated gene fused to a TAP tag (carboxyl-terminal fusion at the endogenous locus) that expressed (+) or not (−) His_8-ubiquitin were treated for 30 min with MG132 (+) or DMSO alone (−). For each set of analyses an equal amount of crude extract protein (8–12 mg) was used for IMAC in buffer containing 8 M urea plus 0.1% SDS. Eluted material was then separated by SDS-PAGE on a 7.5% gel followed by immunoblotting with anti-calmodulin-binding peptide antibody. Only the regions above the unmodified tagged proteins are shown. * denotes experiments that revealed a weak MG132-dependent enrichment. Note that only the signal of Met13-TAP was not increased after the addition of MG132. *Ubi*, ubiquitin.

observed for 17 of the 18 tested candidates (Fig. 2*B*). Notably several proteins with *q* values close to the 0.05 threshold (*e.g.* Rps8A) were shown to accumulate as ubiquitylated species after proteasome inhibition. These data provide strong evidence that the list of proteins derived by our approach is highly enriched for proteasome substrates.

The UPS Proteome—During the course of this study, we acquired an LTQ linear ion trap mass spectrometer that enabled us to obtain quantitative information on more than 500 proteins in a single 10-h analysis (Fig. 3*A*), thereby revealing 225 proteins that were specifically enriched in MG132-treated cells (using the same approach as in Fig. 1; Supplemental Table 6). Thus, 3–4% of all proteins encoded in the yeast genome detectably accumulated as ubiquitylated species when the proteasome was inhibited. Using this more substantial collection of candidate UPS substrates, we performed *in silico* analyses to determine the functions, localization, and expression level of proteins targeted to the UPS. Candidate UPS substrates were distributed across many different functional classes (Fig. 3*B*) with proteins involved in small molecule metabolism accounting for the biggest fraction (24%). Notably we also identified many cell cycle control proteins (10%), including Cdc5, Cdc20, Clb2, Cln1, Cln2, and Far1, which are known substrates of the proteasome (34–38). Com-

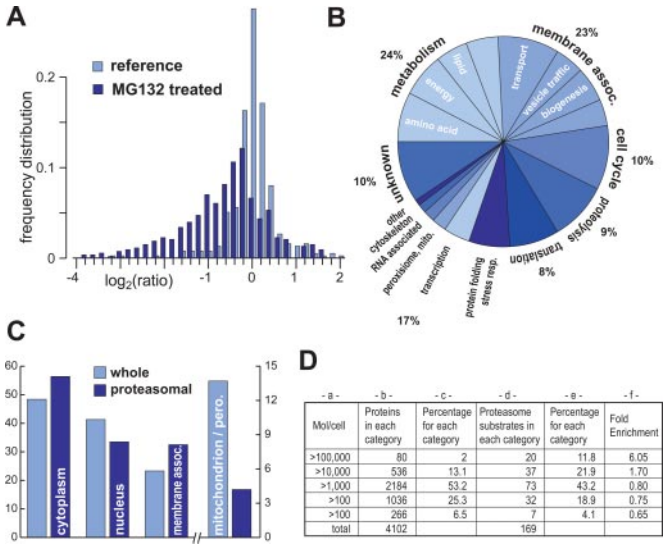

- a - Mol/cell	- b - Proteins in each category	- c - Percentage for each category	- d - Proteasome substrates in each category	- e - Percentage for each category	- f - Fold Enrichment
>100,000	80	2	20	11.8	6.05
>10,000	536	13.1	37	21.9	1.70
>1,000	2184	53.2	73	43.2	0.80
>100	1036	25.3	32	18.9	0.75
>100	266	6.5	7	4.1	0.65
total	4102		169		

FIG. 3. **The UPS proteome.** *A*, frequency distributions of log ratios in the MG132-treated ^{15}N cell experiment (*dark blue*) and reference experiment (*light blue*; see also Fig. 4*A*) using the LTQ ion trap. Truncation of the graph excluded some log ratios with extreme values. *B*, pie diagram representing the distribution of proteasome substrate functions (with indicated percentage). Gene ontologies were retrieved from the *Saccharomyces* Genome Database (www.stanford.edu/Saccharomyces). *C*, histograms representing the percentage of proteins in the whole (*light blue*) and UPS (*dark blue*) proteomes that are localized in one of four major cellular compartments: cytoplasm (cytoplasm, bud, bud neck, microtubule, and actin), nucleus (nucleus, nucleolus, nuclear periphery, spindle pole, and microtubule), membrane-associated organelles (endoplasmic reticulum, Golgi, endosome, vacuole, lipid particle, cell periphery, and punctate composite), and mitochondria plus peroxisomes. Information was retrieved from a global study based on localization of green fluorescent protein fusion proteins expressed from endogenous loci (39). Note that some proteins localized in more than one compartment. *D*, table representing different categories of protein abundances. Protein abundances were retrieved from a previous study based on a genome-wide collection of TAP tagged open reading frames (40), and categories were arbitrarily established using abundance values (*column a*). Of the 4102 proteins that were successfully quantified, the number of proteins in each category is listed (*column b*) as is the percentage of total proteins represented by that category (*column c*). Of the 225 putative UPS substrates identified in the MG132 analysis, 169 were quantified by Ghaemmaghami *et al.* (40). Of these, the total number that fall into each abundance category is listed (*column d*) as is the corresponding percentage (*column e*). *Column f* equals *column e* divided by *column c* and thus represents the degree of enrichment for proteins in each abundance category. *resp.*, response; *mito.*, mitochondria; *pero.*, peroxisomes; *assoc.*, associated.

parison of our dataset with a global green fluorescent protein localization study (39) revealed that UPS substrates were recovered from all major cellular compartments but were notably de-enriched in mitochondria and peroxisomes (Fig. 3*C*). This is not surprising given that there is no known retrotranslocation pathway for the proteasome-dependent degradation of mitochondrial and peroxisomal proteins that are sequestered from the cytoplasm (note that the few identified mitochondrial proteins may have been ubiquitylated prior to their translocation into the organelle). When we assessed the abundance of UPS substrates using a previously reported global analysis of protein expression levels (40), we found that highly abundant proteins ($>10^5$ molecules/cell) were enriched 6-fold in the pool of proteasome substrates (Fig. 3*D*). Although our dataset was slightly biased against proteins present at less than 1000 molecules/cell (*i.e.* 0.7-fold enrichment), we nevertheless detected some of the least abundant yeast proteins, including Gcn4, Ecm3, and Cpr4 (estimated to be present at less than 50 molecules/cell (40)). Taken together, these data indicate that our approach provided a "broad and deep" view of the ubiquitylated proteins that are targeted to the proteasome for degradation regardless of their function, localization, or abundance.

The Rpn10-dependent Ubiquitin Conjugates—Previous studies have resulted in the identification of several ubiquitylated substrates that depend on the proteasome receptor Rpn10 for targeting and degradation (5, 15). However, it is unclear which portion of ubiquitylated proteins is influenced by Rpn10. Given that *rpn10*Δ mutants are viable and have modest phenotypes, it is possible that Rpn10 contributes to the degradation of only a small fraction of proteasome substrates. A competing hypothesis is that Rpn10 contributes to the degradation of a relatively large number of proteasome substrates, but these substrates can use other receptor pathways when Rpn10 is absent. Such substrates might be missed in a subtractive search for substrates that are found uniquely in *rpn10*Δ but not wild-type cells (15) because this type of search is biased toward identifying those substrates that poorly engage an alternative pathway in the absence of Rpn10. However, a quantitative method that can detect changes in accumulation of ubiquitylated proteins might reveal substrates influenced by *RPN10* even if their degradation is only modestly retarded in the absence of Rpn10 due to their ability to engage redundant targeting mechanisms.

To address the question of how many ubiquitylated species exhibit a change in accumulation upon loss of Rpn10, we compared the ubiquitin conjugate proteomes of wild-type and *rpn10*Δ cells. Cells lacking *RPN10* grown in ^{14}N and wild-type cells grown in ^{15}N were mixed together, lysed, and subjected to sequential affinity purification of ubiquitin conjugates followed by MudPIT and quantitative analysis as described in Fig. 1. In this analysis, quantitative information was obtained for 530 proteins (Fig. 4*A*, *middle panel*). We identified 122 proteins that were specifically enriched in *rpn10*Δ cells (Supplemental Fig. 3*A* and Table 7). Among these proteins, both Sic1 and Gcn4, which require *RPN10* for turnover at normal rates (5, 15), were identified. Thus, these proteins serve as internal standards to lend confidence that this approach can successfully identify proteins whose degradation is influenced by *RPN10*. It is important to note that this does not mean that these substrates *depended*, in an absolute sense, upon Rpn10 for their turnover. Rather in the absence of Rpn10, the amount of these substrates that accumulated as ubiquitylated

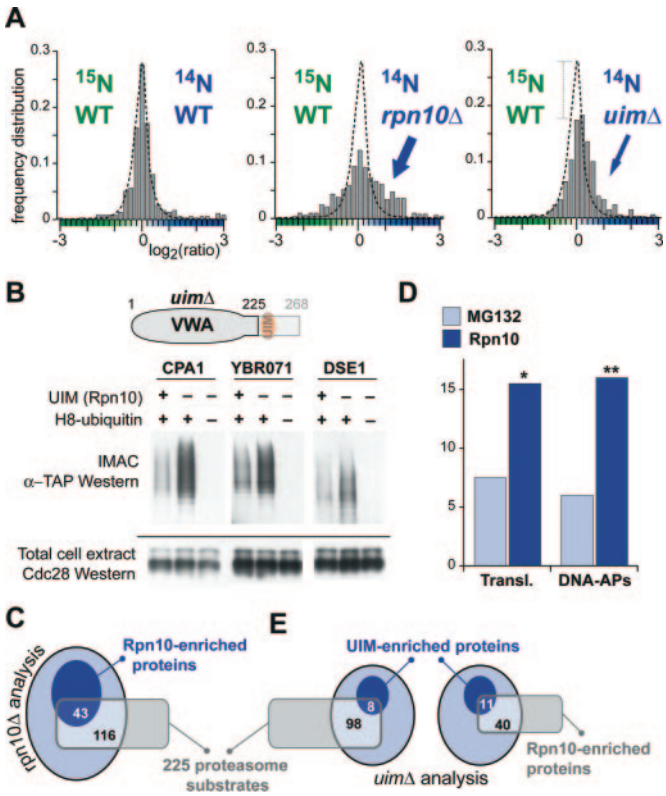

FIG. 4. **Analysis of the impact of Rpn10 on the UPS proteome.** *A*, frequency distributions of log ratios. All analyses were performed using the LTQ ion trap. The reference experiment (displayed on the *left*) was performed by comparing ^{14}N WT *versus* ^{15}N WT cells (370 proteins). Using the same method applied to the reference experiment in Fig. 1, the variance (σ^2) was estimated at 0.46. In the ^{14}N *rpn10*Δ *versus* ^{15}N WT analysis, 530 proteins were quantified (*middle*), and in the ^{14}N *uim*Δ *versus* ^{15}N WT analysis, 344 proteins were quantified (*right*). The bell-shaped distribution obtained in the reference experiment is depicted in the three panels as a *dotted line*. Only frequencies for |log ratio| <3 are shown. *B*, validation of UIM-dependent proteasomal targets. Proteins conjugated to His_8-ubiquitin were purified. Lysates of *RPN10* (+) and *uim*Δ (−) strains with the indicated gene fused to a TAP tag (carboxyl-terminal fusion at the endogenous locus) and that expressed (+) or did not express (−) His_8-ubiquitin were compared. For each set of samples an equal amount of crude extract protein (3–6 mg) was used for IMAC in buffer containing 8 M urea plus 0.1% SDS. Eluted materials were separated by SDS-PAGE on a 4–20% gel followed by immunoblotting with anti-TAP antibody (*top panel*). Total cell extracts were fractionated by SDS-PAGE on a 10% gel followed by immunoblotting with PSTAIRE antibody (*bottom panel*). *C*, analysis of the influence of Rpn10 on the UPS proteome. A Venn diagram representing the overlaps of the 225 proteasomal substrates, depicted in *gray*, with total ubiquitylated proteins identified in the *rpn10*Δ (*light blue*) *versus* those conjugates that accumulated in *rpn10*Δ cells (*dark blue*) is shown. *D*, histogram representing the percentage of proteins functioning in translation (*Transl.*) and DNA-associated proteins (*DNA-APs*) that were enriched in MG132-treated cells (LTQ experiment; *light blue*) or *Rpn10*Δ cells (*dark blue*). The *p* values calculated with Fisher's test were 0.04 and 0.004, respectively. *E*, impact of loss of the UIM domain of Rpn10 on the UPS proteome. Venn diagrams representing the overlaps of the 225 proteasomal substrates (*left*) or 122 proteins enriched in *rpn10*Δ cells (*right*) with proteins identified in the UIM analysis (*light blue*) and proteins specifically enriched in *uim*Δ cells (*dark blue*) are shown.

species was higher. This can be due to several reasons. The most likely is that degradation of the ubiquitylated intermediate was slowed in the absence of Rpn10. However, it is also possible for some substrates that loss of Rpn10 repressed editing by deubiquitylating (DUB) enzymes or increased the rate of ubiquitylation. Regardless of the exact mechanism at play, the quantification approach used here reveals that Rpn10 has a broad impact on the UPS.

Quantitative Analysis of the UIM Domain of Rpn10—We sought to determine whether this approach could also uncover UPS substrates whose metabolism was influenced by the UIM domain of Rpn10. We had previously failed to identify UIM-dependent targets using a subtractive approach.[4] Deletion of UIM yields no known cellular phenotype unless the *uim*Δ mutation is combined with other mutations that compromise the UPS (5). This scenario is compatible with at least two hypotheses. On the one hand, the UIM domain of Rpn10 might only target a small portion of the UPS proteome. Alternatively the UIM domain might not be involved in substrate degradation unless other targeting mechanisms are compromised.

To address the role of the UIM domain, we compared the ubiquitin conjugate proteomes of wild-type and *uim*Δ cells. Mutant *uim*Δ cells grown in ^{14}N and wild-type cells grown in ^{15}N were processed as for the *RPN10* analysis (Fig. 4*A*, *right panel*). We found that the distribution of log ratios, when compared with that obtained in the reference experiment, exhibited a shift to the right and increased spread but to a much lesser extent than that seen in the *RPN10* and MG132 analyses. We performed a reciprocal experiment to ensure that this increase was specific to the UIM deletion and found a very similar result (data not shown). Our results suggest the existence of specific proteins that accumulate as ubiquitin conjugates when the UIM domain is mutated. Because the perturbation was relatively subtle ($1 - \pi_0 = 15\%$), low *q* value thresholds (*e.g.* 0.05) were associated with poor recovery rates (Supplemental Fig. 3A). Hence in this particular case, we used a less restrictive threshold (<0.15) to increase the recovery rate (>75%). Among the 35 proteins that specifically accumulated in *uim*Δ cells (Supplemental Table 8), we selected three candidate genes for validation according to their availability (*CPA1*, *DSE1*, and *YBR071W*). Using the same approach as in Fig. 2*A*, we were able to confirm an increase of ubiquitin conjugate levels in *uim*Δ cells for these three candidates (Fig. 4*B*; note that both *DSE1* and *YBR071W* have *q* values between 0.1 and 0.15). To date, no such protein has ever been described. This result illustrates the ability of shotgun-based isotopic quantification to identify UPS substrates whose metabolism is influenced by a particular functional element (*i.e.* the UIM domain of Rpn10) even when mutation of that element has little or no discernable phenotype.

Proportional Impact of the Rpn10 Deletion on Proteasome

[4] T. Mayor and R. J. Deshaies, unpublished data.

Substrates—To gain a better idea of how broad a contribution Rpn10 makes to the operation of the UPS, we sought to determine what fraction of UPS substrates identifiable by our method (*i.e.* those conjugates that accumulated upon treatment of cells with MG132) also accumulated upon deletion of *RPN10*. The estimated proportion of proteins affected by the loss of *RPN10* ($1 - \pi_0 = 45\%$) is lower than in MG132-treated cells (Fig. 3*A*; $1 - \pi_0 = 75\%$). This indicates that, on a proteome-wide level, the loss of *RPN10* has less impact on polyubiquitylated proteins than does inhibition of the proteasome. This is not surprising given the existence of multiple receptors that guide ubiquitylated proteins to the proteasome. To identify the UPS substrates whose degradation is influenced by *RPN10*, we focused on the 225 proteins enriched in MG132-treated cells (Supplemental Table 6) and evaluated their enrichment in the *rpn10*Δ analysis. Among the 225 ubiquitylated species that accumulated in MG132-treated cells, 159 were also present in the *rpn10*Δ *versus* WT analysis, including 43 proteins that were enriched in the mutant cells (Fig. 4*C*). This degree of overlap (159/225 = 70%) is anticipated by the observation that any single MudPIT run reveals ~⅔ of the identifiable proteins in a complex sample (41). This result suggests that metabolism of 27% (43 of 159) of all UPS substrates detectable in the two separate analyses was influenced by Rpn10 (Fig. 4*C*).

To further address whether a particular class of substrates was specifically affected by Rpn10 absence, we compared the distributions of the different functional classes. As in the previously analysis (Fig. 3*B*), a large array of classes were represented among the proteins enriched in *Rpn10*Δ cells, suggesting a broad function of Rpn10 in the UPS (Supplemental Fig. 3B). However, some variations could be observed when the two analyses were compared (*RPN10 versus* MG132). Notably fewer proteins associated to small molecule metabolism were identified in *rpn10*Δ cells (Supplemental Fig. 3B). Concurrently the proportions of proteins functioning in translation and DNA-associated proteins were significantly enhanced (Fig. 4*D*). This suggests that Rpn10 may be more important for the degradation of that particular subset of ubiquitylated proteasome substrates.

Proportional Impact of the UIM Domain—We next performed a comparative analysis, as for the prior analysis of *rpn10*Δ, to gauge the influence of the UIM domain of Rpn10 on UPS substrates. In this case, of the 225 putative UPS substrates found to accumulate in the MG132 experiment, 106 were detected in the *uim*Δ *versus* WT analysis. Of these, only eight were enriched in *uim*Δ cells, representing ~7.5% (8 of 106) of the UPS-pooled substrates (Fig. 4*E*, *left diagram*). This shows that deletion of the UIM domain has far less impact than deletion of *RPN10*. Indeed when we considered the overlap between the *RPN10* and UIM analysis, only about 22% of proteins enriched in *rpn10*Δ cells were also enriched in *uim*Δ cells (11 of 51; Fig. 4*E*, *right diagram*). The implication of this result is that, of the UPS substrates influenced by Rpn10, only about one-fifth are sensitive to loss of the UIM domain. This shows that Rpn10 functions on different pools of proteasome substrates using two distinctive mechanisms. The dominant function of Rpn10 is provided by the VWA domain that does not directly bind to ubiquitin, whereas the UIM domain, which can bind to polyubiquitin chains, targets a smaller portion of proteasome substrates.

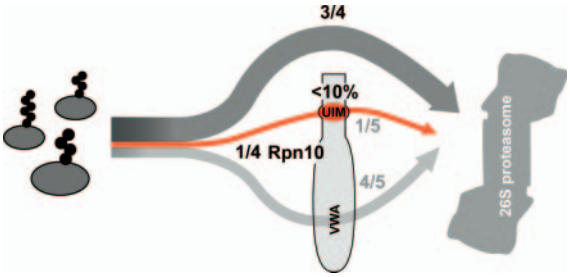

FIG. 5. **Proteasome substrates using Rpn10 pathway.** Schematic representation of the "flux" of UPS substrates using the indicated pathways. Estimates of total proteasome substrate fractions are depicted in *black*, whereas Rpn10 target distributions influenced by the UIM or VWA domains are shown in *gray*.

DISCUSSION

We performed quantitative analysis using ^{15}N metabolic labeling to measure variations in levels of ubiquitin conjugates after chemical and genetic perturbations. In a first series of experiments, we were able to specifically identify UPS substrates using the proteasome inhibitor MG132. We then extended our analysis to identify ubiquitylated proteins that are affected by the Rpn10 pathway. This enabled the identification of several ubiquitylated substrates whose metabolism is influenced by the UIM domain of Rpn10. Finally we compared the different analyses to gauge the relative impact of deleting sequences encoding either the entire *RPN10* or only its UIM domain on the UPS proteome.

The Rpn10 Pathway—By comparing datasets for ubiquitin conjugates that accumulate when the proteasome is inhibited with MG132 (putative UPS substrates) and those that accumulate in *rpn10*Δ cells, we estimated that Rpn10 influenced the steady-state level of ubiquitin conjugates for up to ~27% of all UPS substrates (Fig. 5). The simplest interpretation of this result is that Rpn10 contributes to the turnover of a significant number of ubiquitylated proteins. However, we cannot exclude the possibility that in some cases the role of Rpn10 in turnover is indirect or that the increase in conjugates is due to increased ubiquitylation or decreased deubiquitylation. Interestingly there were also several proteins that were significantly de-enriched in *rpn10*Δ cells suggesting that Rpn10 function might be broader than suspected. Given that *rpn10*Δ cells exhibit mild phenotypes (12) this important impact of *rpn10*Δ in our experiments is somewhat surprising. Presumably the "Rpn10-dependent" candidate substrates reported here do not rely exclusively on Rpn10 for delivery to the proteasome. Instead it is more likely that substrates that

use Rpn10 can also use other receptor pathways, albeit with reduced overall efficiency, when Rpn10 is absent as is the case for Sic1 (5).

The role of the UIM domain of Rpn10 in the UPS has been perplexing. Although it was the first polyubiquitin binding domain to be identified, it remained unclear whether it plays any role in proteolysis in wild-type cells. The Rpn10-dependent substrates Sic1 and Gcn4 are unaffected by the UIM deletion unless it is combined with deletions of other receptors such as *RAD23* (5).[2] In this analysis we identified several ubiquitylated substrates that accumulated in *uim*Δ cells (Supplemental Table 8). To our knowledge, these represent the first physiological UPS substrates that have been shown to be affected by loss of the UIM domain by itself. This shows that there is a dual role for Rpn10 function at the proteome-wide level (Fig. 5). Those identified proteins can now be used as "indicator proteins" to unravel the physiological role of the UIM domain. The notion of using mass spectrometry to identify an "indicator protein" should be readily applicable to other poorly understood components of the UPS.

Of the proteins accumulating as ubiquitylated species upon *RPN10* deletion, only one-fifth accumulated upon the selective deletion of the UIM domain. This is consistent with the observation that *rpn10*Δ cells have a more severe growth defect than *uim*Δ cells (12). The substrates that accumulated in *rpn10*Δ but not *uim*Δ cells presumably are dependent upon the VWA domain. The VWA domain enhances the degradation of ubiquitylated Sic1 docked to the proteasome by the Rad23 receptor, but the biochemical function of the VWA domain remains unknown. Interestingly ribosome and DNA-associated proteins were found to be significantly enriched in the Rpn10 analysis but not in the UIM analysis (data not shown). These proteins are part of large and tight complexes. It is possible that the VWA might participate in the structural conformation of the 19 S subunit of the proteasome, favoring a larger entry site for the substrate or better alignment with other proteasomal functions (*e.g.* Rpn11-DUB or the chaperone activities of Rpt).

The UPS Proteome—Our analysis revealed a large number of ubiquitylated proteins that accumulated upon inhibition of the proteasome, including relatively low abundance cell cycle control proteins whose activity is known to be regulated by proteolysis (G_1 cyclins Cln1, Cln2, and Pcl1; B-type cyclin Clb2; and Cdk inhibitors Sic1 and Far1). Interestingly we also found and confirmed that abundant, presumably stable proteins (ribosomal protein Rps8A, enolase, and phosphoglycerate kinase) accumulated as ubiquitylated species upon inhibition of the proteasome with MG132 (Fig. 2*B*). It is possible that these proteins succumbed to quality control mechanisms that eliminate improperly translated, misfolded, or damaged proteins (42, 43). If so, the methods reported here may be useful for studying on a proteome-wide scale the chaperones involved in protein folding and assembly. An important feature of our method is that we use consecutive affinity purification steps to focus our analysis on proteasome substrates and bias against contaminating proteins. The effectiveness of this strategy is underscored by the fact that >22% of our candidate UPS substrates are present at <1000 molecules/cell, whereas only 6.8% of proteins identified in a single MudPIT analysis of crude extract are of equivalent abundance (41). The positive attributes of this method suggest that it should be generally useful for identifying targets of specific ubiquitin ligases and deubiquitylating enzymes.

General Issues in Quantitative Profiling of UPS Substrates—The accumulation of a particular substrate in any given experiment was likely guided by several factors, including the amount of co-accumulating substrates, the relative activity of individual ubiquitin ligases and DUB enzymes that act upon the substrate, the relative ability of different ubiquitylation pathways to incorporate His_6-ubiquitin or compete for free ubiquitin, and the degradation rate of the ubiquitylated protein. Because of these factors, we believe there is little value in investing great significance in individual ratios when drawing conclusions in a proteomics manner. Thus, we limited our analysis to classifying proteins as being enriched or not.

In many cases the enrichment values for UPS substrates were lower than the threshold of 4 (or 2 when expressed in $\log_2$ scale) often applied in microarray analyses of mRNA expression (44). In our experiments, the total enrichment for ubiquitin recovered from MG132-treated compared with untreated cells averaged only ~1.9-fold (in Fig. 1). Thus, one would expect the average ubiquitylated substrate to accumulate 2–3-fold. This value agrees with immunoblot analysis of ubiquitin conjugates in total cell extracts. Although we could have increased this value by longer treatment with MG132, excessive accumulation of conjugates runs the risk of depleting cellular ubiquitin, thereby causing its redistribution to different proteins (45, 46). Remarkably despite the limited extent of accumulation of total ubiquitin conjugates, large variations in accumulation of specific conjugates were seen.

We used a statistical analysis based on *q* values to identify proteins for which the ubiquitylation level was altered. The reference experiment, in which two biologically equivalent pools were compared, provided crucial information regarding the typical variation arising from simple biological variability and experimental noise. Protein-specific *p* values provide a statistical measure of the inconsistency between the observed log ratio and a null hypothesis of no enrichment or depletion. We further modified our *p* values prior to forming lists to address the perennial problem in "omic" analyses, namely the large scale multiple testing problem. A simple filter for *p* values only allows a selection based on the error rate (proportion of unaffected ORFs that are considered enriched, *i.e.* false negative), whereas *q* values allow the setting of a threshold FDR (based on false positive rate). By setting a *q* value threshold of 0.05 (or 0.15 in the UIM analysis), the lists of putative proteome substrates have, on average, a false positive proportion smaller than 5% (or 15%). Note that in all

experiments the error rates were below or close to 10%. In addition to the absolute meaning of the *q* value cutoff in terms of the FDR, our choice of cutoff was guided by a desire to recover a high proportion (which we estimated to be close to 80% in most of our analyses) of the ORFs that responded to a chemical (MG132) or genetic (*rpn10*Δ, *uim*Δ) perturbation of the UPS. Manual validation of a subset of proteins from the MG132 and *uim*Δ analyses confirmed the efficacy of the approach. To our best knowledge, this is the first analysis that combines the null distribution of a reference experiment and *q* value test to identify responsive or affected proteins in quantitative mass spectrometry analysis. This method offers considerable promise that could be broadly applied to other proteomics studies.

Acknowledgments—We thank Brian Williams for help in the list analysis and Barbara J. Wold, Rati Verma, Robert Riley, Sonja Hess, Allan D. Drummond, and Kenneth McCue for discussion. We thank all current and past members of the Deshaies laboratory for help, in particular Geoff T. Smith for dedicated technical assistance. T. M. also thanks Gary Kleiger for discussions, encouragement, and shared coffee breaks.

* This work was supported in part by the Howard Hughes Medical Institute. The costs of publication of this article were defrayed in part by the payment of page charges. This article must therefore be hereby marked "*advertisement*" in accordance with 18 U.S.C. Section 1734 solely to indicate this fact.

S The on-line version of this article (available at http://www.mcponline.org) contains supplemental material.

¶ To whom correspondence should be addressed: Dept. of Biochemistry and Molecular Biology, UBC Centre for Proteomics, University of British Columbia, 301-2185 East Mall, Vancouver, British Columbia V6T 1Z4, Canada. Tel.: 604-822-5144; Fax: 604-822-2114; E-mail: mayor@interchange.ubc.ca.

** Supported by Natural Sciences and Engineering Research Council (Canada) and the Michael Smith Foundation for Health Research.

§§ Supported by National Institutes of Health Grant P41-RR011823.

¶¶ An Investigator of the Howard Hughes Medical Institute.

REFERENCES

1. Madura, K. (2004) Rad23 and Rpn10: perennial wallflowers join the melee. *Trends Biochem. Sci.* **29,** 637–640
2. Elsasser, S., Chandler-Militello, D., Muller, B., Hanna, J., and Finley, D. (2004) Rad23 and Rpn10 serve as alternative ubiquitin receptors for the proteasome. *J. Biol. Chem.* **279,** 26817–26822
3. Ivantsiv, Y., Kaplun, L., Tzirkin-Goldin, R., Shabek, N., and Raveh, D. (2006) Unique role for the UbL-UbA protein Ddi1 in turnover of SCFUfo1 complexes. *Mol. Cell. Biol.* **26,** 1579–1588
4. Medicherla, B., Kostova, Z., Schaefer, A., and Wolf, D. H. (2004) A genomic screen identifies Dsk2p and Rad23p as essential components of ER-associated degradation. *EMBO Rep.* **5,** 692–697
5. Verma, R., Oania, R., Graumann, J., and Deshaies, R. J. (2004) Multiubiquitin chain receptors define a layer of substrate selectivity in the ubiquitin-proteasome system. *Cell* **118,** 99–110
6. Lam, Y. A., Lawson, T. G., Velayutham, M., Zweier, J. L., and Pickart, C. M. (2002) A proteasomal ATPase subunit recognizes the polyubiquitin degradation signal. *Nature* **416,** 763–767
7. Hartmann-Petersen, R., Wallace, M., Hofmann, K., Koch, G., Johnsen, A. H., Hendil, K. B., and Gordon, C. (2004) The Ubx2 and Ubx3 cofactors direct Cdc48 activity to proteolytic and nonproteolytic ubiquitin-dependent processes. *Curr. Biol.* **14,** 824–828
8. Deveraux, Q., Ustrell, V., Pickart, C., and Rechsteiner, M. (1994) A 26 S protease subunit that binds ubiquitin conjugates. *J. Biol. Chem.* **269,** 7059–7061
9. Hofmann, K., and Falquet, L. (2001) A ubiquitin-interacting motif conserved in components of the proteasomal and lysosomal protein degradation systems. *Trends Biochem. Sci.* **26,** 347–350
10. Hiyama, H., Yokoi, M., Masutani, C., Sugasawa, K., Maekawa, T., Tanaka, K., Hoeijmakers, J. H., and Hanaoka, F. (1999) Interaction of hHR23 with S5a. The ubiquitin-like domain of hHR23 mediates interaction with S5a subunit of 26 S proteasome. *J. Biol. Chem.* **274,** 28019–28025
11. van Nocker, S., Sadis, S., Rubin, D. M., Glickman, M., Fu, H., Coux, O., Wefes, I., Finley, D., and Vierstra, R. D. (1996) The multiubiquitin-chain-binding protein Mcb1 is a component of the 26S proteasome in Saccharomyces cerevisiae and plays a nonessential, substrate-specific role in protein turnover. *Mol. Cell. Biol.* **16,** 6020–6028
12. Fu, H., Sadis, S., Rubin, D. M., Glickman, M., van Nocker, S., Finley, D., and Vierstra, R. D. (1998) Multiubiquitin chain binding and protein degradation are mediated by distinct domains within the 26 S proteasome subunit Mcb1. *J. Biol. Chem.* **273,** 1970–1981
13. Kirkpatrick, D. S., Weldon, S. F., Tsaprailis, G., Liebler, D. C., and Gandolfi, A. J. (2005) Proteomic identification of ubiquitinated proteins from human cells expressing His-tagged ubiquitin. *Proteomics* **5,** 2104–2111
14. Matsumoto, M., Hatakeyama, S., Oyamada, K., Oda, Y., Nishimura, T., and Nakayama, K. I. (2005) Large-scale analysis of the human ubiquitin-related proteome. *Proteomics* **5,** 4145–4151
15. Mayor, T., Lipford, J. R., Graumann, J., Smith, G. T., and Deshaies, R. J. (2005) Analysis of polyubiquitin conjugates reveals that the Rpn10 substrate receptor contributes to the turnover of multiple proteasome targets. *Mol. Cell. Proteomics* **4,** 741–751
16. Peng, J., Schwartz, D., Elias, J. E., Thoreen, C. C., Cheng, D., Marsischky, G., Roelofs, J., Finley, D., and Gygi, S. P. (2003) A proteomics approach to understanding protein ubiquitination. *Nat. Biotechnol.* **21,** 921–926
17. Tagwerker, C., Flick, K., Cui, M., Guerrero, C., Dou, Y., Auer, B., Baldi, P., Huang, L., and Kaiser, P. A. (2006) A tandem affinity tag for two-step purification under fully denaturing conditions: application in ubiquitin profiling and protein complex identification combined with in vivo cross-linking. *Mol. Cell Proteomics* **5,** 737–748
18. Hitchcock, A. L., Auld, K., Gygi, S. P., and Silver, P. A. (2003) A subset of membrane-associated proteins is ubiquitinated in response to mutations in the endoplasmic reticulum degradation machinery. *Proc. Natl. Acad. Sci. U. S. A.* **100,** 12735–12740
19. Chi, Y., Huddleston, M. J., Zhang, X., Young, R. A., Annan, R. S., Carr, S. A., and Deshaies, R. J. (2001) Negative regulation of Gcn4 and Msn2 transcription factors by Srb10 cyclin-dependent kinase. *Genes Dev.* **15,** 1078–1092
20. Andrews, P., He, Y. J., and Xiong, Y. (2006) Cytoplasmic localized ubiquitin ligase cullin 7 binds to p53 and promotes cell growth by antagonizing p53 function. *Oncogene* **25,** 4534–4548
21. Brooks, C. L., and Gu, W. (2006) p53 ubiquitination: Mdm2 and beyond. *Mol. Cell* **21,** 307–315
22. Grossman, S. R., Deato, M. E., Brignone, C., Chan, H. M., Kung, A. L., Tagami, H., Nakatani, Y., and Livingston, D. M. (2003) Polyubiquitination of p53 by a ubiquitin ligase activity of p300. *Science* **300,** 342–344
23. Mayor, T., and Deshaies, R. J. (2005) Two-step affinity purification of multiubiquitylated proteins from Saccharomyces cerevisiae. *Methods Enzymol.* **399,** 385–392
24. Fleming, J. A., Lightcap, E. S., Sadis, S., Thoroddsen, V., Bulawa, C. E., and Blackman, R. K. (2002) Complementary whole-genome technologies reveal the cellular response to proteasome inhibition by PS-341. *Proc. Natl. Acad. Sci. U. S. A.* **99,** 1461–1466
25. Wessel, D., and Flugge, U. I. (1984) A method for the quantitative recovery of protein in dilute solution in the presence of detergents and lipids. *Anal. Biochem.* **138,** 141–143
26. Graumann, J., Dunipace, L. A., Seol, J. H., McDonald, W. H., Yates, J. R., III, Wold, B. J., and Deshaies, R. J. (2004) Applicability of tandem affinity purification MudPIT to pathway proteomics in yeast. *Mol. Cell. Proteomics* **3,** 226–237
27. Eng, J. K., McCormack, A. L., and Yates, J. R., III (1994) An approach to correlate tandem mass-spectral data of peptides with amino-acid-sequences in a protein database. *J. Am. Soc. Mass Spectrom.* **5,** 976–989
28. Tabb, D. L., McDonald, W. H., and Yates, J. R., III (2002) DTASelect and Contrast: tools for assembling and comparing protein identifications

from shotgun proteomics. *J. Proteome Res.* **1,** 21–26
29. MacCoss, M. J., Wu, C. C., Liu, H., Sadygov, R., and Yates, J. R., III (2003) A correlation algorithm for the automated quantitative analysis of shotgun proteomics data. *Anal. Chem.* **75,** 6912–6921
30. Benjamini, Y., and Hochberg, Y. (1995) Controlling the false discovery rate—a practical and powerful approach to multiple testing. *J. R. Stat. Soc. Ser. B Stat. Methodol.* **57,** 289–300
31. Storey, J. D., and Tibshirani, R. (2003) Statistical significance for genome-wide studies. *Proc. Natl. Acad. Sci. U. S. A.* **100,** 9440–9445
32. Ong, S. E., and Mann, M. (2005) Mass spectrometry-based proteomics turns quantitative. *Nat. Chem. Biol.* **1,** 252–262
33. Washburn, M. P., Wolters, D., and Yates, J. R., III (2001) Large-scale analysis of the yeast proteome by multidimensional protein identification technology. *Nat. Biotechnol.* **19,** 242–247
34. Deshaies, R. J., Chau, V., and Kirschner, M. (1995) Ubiquitination of the G1 cyclin Cln2p by a Cdc34p-dependent pathway. *EMBO J.* **14,** 303–312
35. Zachariae, W., and Nasmyth, K. (1996) TPR proteins required for anaphase progression mediate ubiquitination of mitotic B-type cyclins in yeast. *Mol. Biol. Cell* **7,** 791–801
36. Henchoz, S., Chi, Y., Catarin, B., Herskowitz, I., Deshaies, R. J., and Peter, M. (1997) Phosphorylation- and ubiquitin-dependent degradation of the cyclin-dependent kinase inhibitor Far1p in budding yeast. *Genes Dev.* **11,** 3046–3060
37. Prinz, S., Hwang, E. S., Visintin, R., and Amon, A. (1998) The regulation of Cdc20 proteolysis reveals a role for APC components Cdc23 and Cdc27 during S phase and early mitosis. *Curr. Biol.* **8,** 750–760
38. Shirayama, M., Zachariae, W., Ciosk, R., and Nasmyth, K. (1998) The Polo-like kinase Cdc5p and the WD-repeat protein Cdc20p/fizzy are regulators and substrates of the anaphase promoting complex in Saccharomyces cerevisiae. *EMBO J.* **17,** 1336–1349
39. Huh, W. K., Falvo, J. V., Gerke, L. C., Carroll, A. S., Howson, R. W., Weissman, J. S., and O'Shea, E. K. (2003) Global analysis of protein localization in budding yeast. *Nature* **425,** 686–691
40. Ghaemmaghami, S., Huh, W. K., Bower, K., Howson, R. W., Belle, A., Dephoure, N., O'Shea, E. K., and Weissman, J. S. (2003) Global analysis of protein expression in yeast. *Nature* **425,** 737–741
41. Liu, H., Sadygov, R. G., and Yates, J. R., III (2004) A model for random sampling and estimation of relative protein abundance in shotgun proteomics. *Anal. Chem.* **76,** 4193–4201
42. McClellan, A. J., Tam, S., Kaganovich, D., and Frydman, J. (2005) Protein quality control: chaperones culling corrupt conformations. *Nat. Cell. Biol.* **7,** 736–741
43. Princiotta, M. F., Finzi, D., Qian, S. B., Gibbs, J., Schuchmann, S., Buttgereit, F., Bennink, J. R., and Yewdell, J. W. (2003) Quantitating protein synthesis, degradation, and endogenous antigen processing. *Immunity* **18,** 343–354
44. Hoheisel, J. D. (2006) Microarray technology: beyond transcript profiling and genotype analysis. *Nat. Rev. Genet.* **7,** 200–210
45. Mimnaugh, E. G., Chen, H. Y., Davie, J. R., Celis, J. E., and Neckers, L. (1997) Rapid deubiquitination of nucleosomal histones in human tumor cells caused by proteasome inhibitors and stress response inducers: effects on replication, transcription, translation, and the cellular stress response. *Biochemistry* **36,** 14418–14429
46. Dantuma, N. P., Groothuis, T. A., Salomons, F. A., and Neefjes, J. (2006) A dynamic ubiquitin equilibrium couples proteasomal activity to chromatin remodeling. *J. Cell Biol.* **173,** 19–26